CMLS, Cell. Mol. Life Sci. 61 (2004) 2264–2273
1420-682X/04/172264-10
DOI 10.1007/s00018-004-4205-x

CMLS Cellular and Molecular Life Sciences

Research Article

Hcc-1 is a novel component of the nuclear matrix with growth inhibitory function

C. L. Leaw [a, b], E. C. Ren [b] and M. L. Choong [a, c, *]

[a] Bioprocessing Technology Institute, Agency for Science, Technology and Research (A*STAR) (Singapore)
[b] Department of Microbiology, National University of Singapore (Singapore)
[c] Present address: W.H.O. Collaborating Centre for Research and Training in Immunology, National University of Singapore, Block MD4, 5 Science Drive 2, 117597 Singapore, Fax: +65 6777 5720, e-mail: whocml@nus.edu.sg

Received 13 May 2004; received after revision 30 June 2004; accepted 6 July 2004

Abstract. Hcc-1 is a novel nuclear protein containing the SAF-box DNA-binding domain. It binds to both double-stranded and single-stranded DNA with higher affinity for the single-stranded form. In addition, it also binds specifically to scaffold/matrix attachment region DNA. These nucleic acid-binding characteristics suggest a potential function for Hcc-1 as a component of the heterogeneous ribonucleoprotein complex. Using a yeast two-hybrid screen, two DEAD-box RNA helicases, BAT1 and DDX39, were identified as proteins that interact with Hcc-1. Interactions with these RNA helicases suggested a role for Hcc-1 in nucleic acid biogenesis. Expression of Hcc-1 in the HEK293 cell line resulted in a slower growth rate compared to controls ($p = 0.0173$) and an accumulation of cells at the G2/M phase ($p = 0.0276$ compared to control HEK293 cells). Taken together, these results suggest a role for Hcc-1 in growth regulation and nucleic acids metabolism.

Key words. DEAD-box family; heterogeneous ribonucleoprotein; nuclear matrix protein; SAF-box; scaffold attachment region DNA.

Hcc-1 is a novel nuclear protein with no homology to any known proteins when it was first identified by a proteome analysis of the hepatocellular carcinoma (HCC)-M cell line [1]. The level of *Hcc-1* mRNA was shown to be elevated in well-differentiated HCC, pancreatic adenocarcinoma, some solid tumors, myeloid leukemia and lymphoma cell lines, suggesting that Hcc-1 may play important cellular roles contributing to tumorigenesis [1, 2]. Hcc-1 is also known under two other names: the proliferation-associated cytokine-inducible protein 29 kDa (CIP29) [2] and HSPC316.

Hcc-1 contains an evolutionarily conserved N-terminal SAP domain [named after the scaffold attachment factor A/B (SAF-A/B), Acinus and poly(ADP-ribose) polymerase proteins] [3] or SAF-box [4]. Several SAP- or SAF-box-containing proteins have been identified and characterized in recent years [5–8]. All these proteins contain a 35-residue conserved motif with a bipartite distribution of strongly conserved hydrophobic, polar and bulky amino acids separated by a region that contains an invariant glycine. These proteins contain a potential DNA-binding motif that could perform a specific role in chromosomal organization and provide links between transcription, repair, RNA processing and apoptotic chromatin degradation. Of particular interest is the consistent association of the N-terminal SAF-box motif with different domains involved in the assembly of RNA-processing complexes. These include the SplA ryanodine receptor (SPRY) domain, polynucleotide-kinase-like ATP-binding domain and RGG repeats in SAF-A/heterogeneous ribonucleoprotein U (hnRNP-U), and the RNA recognition motif (RRM) domain in SAF-B and Acinus [reviewed in ref. 3].

* Corresponding author.

One of the well-characterized SAF-box proteins, SAF-A/hnRNP U, is a nuclear matrix protein that binds to both DNA and RNA [9–11], and scaffold attachment region (SAR) DNA [12]. SAR DNA is a stretch of AT-rich residues located in the intronic regions of DNA and regions that flank functional genes. Attachment of chromatin to the nuclear scaffold seems to occur via these specialized AT-rich DNA elements that have been found in all eukaryotic organisms investigated. Also known as the matrix attachment region, SAR DNA elements are bound by nuclear scaffolds in an evolutionarily conserved manner, presumably because of one or more conserved binding proteins present in these scaffolds. The recognition of SAR DNA by cognate binding proteins apparently does not depend on a precise recognition sequence because a consensus sequence common to all SAR DNA has not been identified. Instead, they may be recognized by structural features and/or short sequence motifs clustered in SAR but not non-SAR DNA [4]. SAR DNA has been proposed to partition the genome into distinct, topologically independent loops of variable size. It is implicated in gene expression regulation by controlling chromatin accessibility [13], and in the maintenance of nuclear architecture via interactions with nuclear matrix proteins (NMPs) [14]. NMPs, together with histones, hnRNPs and SAR DNA are the major constituents of the nuclear matrix, where a wide array of processes such as transcription, DNA replication, gene expression, chromatin modification and RNA splicing take place. In addition, hnRNPs have been shown to be involved in spliceosome assembly by forming spliceosome complexes [15, 16]. Spliceosome assembly is an energy-consuming process where the hydrolysis of ATP is provided by a group of proteins belonging to the DEAD-box family. A recent study has also shown that human prespliceosome-associated proteins consist of U1 and U2 snRNPs, DEAD-box proteins and SAF-box proteins [17].

From our preliminary work on Hcc-1, we hypothesize that it is a novel NMP with a role in nucleic acid metabolism. With this hypothesis, we set out to study the nucleic acid-binding capability of Hcc-1, to identify its potential interacting partners using the yeast two-hybrid assay and to study its functional roles by expressing Hcc-1 in cells that do not express the protein in its natural state. Our results showed that Hcc-1 binds to both double-stranded (ds) and single-stranded (ss) DNA, but shows higher affinity for ssDNA. In addition, it also possesses high specificity toward SAR DNA. Further experiments showed that it interacts with two DEAD-box proteins and overexpression of this protein in HEK293 cells led to growth inhibition, which appeared to be caused by an arrest at the G2/M phase.

Materials and methods

Hcc-1 vector constructs and recombinant protein expression

For the DNA-binding assay, three different fragments of *Hcc-1* [full-length *Hcc-1* (amino acids 1–210), the SAF-box (amino acids 1–58) only, and truncated *Hcc-1* with deletion of the SAF-box, ΔSAF-box (amino acids 59–210)] were cloned into the pGEX-4T1 bacterial expression vector containing a glutathione S-transferase (*GST*) gene (Amersham Biosciences). The full-length and truncated Hcc-1 were expressed in *Escherichia coli* BL21 (DE3) by IPTG induction. The expressed proteins were purified by affinity chromatography using gluthatione-agarose beads (Sigma) according to the protocol described in the GST purification module (Amersham Biosciences). *Hcc-1* with deletion of the SAF-box, ΔSAF-Box (amino acids 43–210), was also cloned into the pGBKT7 (BD Biosciences Clontech) yeast expression vector to generate the pGBKT7-ΔSAF-box for a yeast two-hybrid assay. To verify the yeast two-hybrid assay results, the full-length coding region of the interacting proteins, BAT1 and DDX39, were cloned into the pQE30 expression vector (Qiagen) to generate 6 × His tag fusion proteins. The 6 × His tag fusion proteins were expressed in *E. coli* M15 (pREP4) and purified using Ni-NTA as recommended by the manufacturer (Qiagen). For the co-immunoprecipitation assay, the coding region of BAT1 and DDX39 were cloned into the pCMV-myc (BD Biosciences Clontech) to generate myc fusion proteins. The full-length cDNA sequence of *Hcc-1* was cloned into the pcDNA3.1(+) expression vector (Invitrogen) to generate pcDNA3.1(+)-Hcc-1 for cell proliferation and co-immunoprecipitation assays. The DNA sequences and reading frames of each construct were verified by DNA sequencing on an ABI PRISM 377 sequencer (Applied Biosystems). All purified proteins were quantified by the Coomassie Plus Protein Assay (Pierce) and separated by electrophoresis on 12% SDS-polyacrylamide gels.

Double-stranded and single-stranded DNA cellulose binding assays

Equal amounts (1 mg) of purified GST and GST fused-Hcc-1 proteins (GST-Hcc-1, GST-ΔSAF-box and GST-SAF-box) were applied onto individual ssDNA and ds-DNA cellulose (Sigma) columns that had previously been equilibrated in a binding buffer (50 mM Tris-Cl, pH 7.4, 5 mM $MgCl_2$, 0.5 mM EDTA, 0.1% Igepal). The columns were then washed extensively with the binding buffer. Bound proteins were eluted with 0.05, 0.1, 0.25 and 0.5 M NaCl in the binding buffer. Eluted proteins from each NaCl preparation were separated by SDS-PAGE and visualized by staining with the Coomassie blue dye.

SAR DNA-binding assay

Human SAR DNA (MII) cloned into a pUC18 plasmid was provided by Prof. F. O. Fackelmayer from Heinrich-Pette-Institute, Germany. The MII fragment (2.9 kb) was isolated from the intronic sequence of the human DNA topoisomerase I gene (*TOP1*) [18]. The SAR DNA-binding assay was performed as described previously [4] with minor modifications. Briefly, purified GST-Hcc-1 protein (100 µg) was coupled to glutathione-agarose beads (Sigma) in a binding buffer (100 mM Tris-Cl, pH 7.5, 100 mM NaCl, 1 mM EDTA). Digested pUC18-MII plasmid (250 ng) labeled with digoxigenin (DIG) (Roche Applied Science) was added to the settled glutathione-agarose beads in the binding buffer and incubated for 1 h. Sheared *E. coli* DNA (ICN) and chromomycin (Sigma) were used as non-specific competitors, while poly-dA-dT (Roche Applied Science) and distamycin (Sigma) were used as specific competitors. Unbound DNA was removed by washing three times with the binding buffer. Bound DNA retained in the column was eluted from the glutathione-agarose beads in the same binding buffer containing 3% SDS. TE buffer (pH 8.0) was then added immediately to the eluent. DNA was purified by phenol-chloroform extraction and ethanol precipitation. The purified DNA was then Southern transferred to a nitrocellulose membrane (Amersham Biosciences) and detected with an anti-DIG antibody (Roche Applied Science).

Yeast two-hybrid assay

Yeast two-hybrid assay was performed using the MATCHMAKER two-hybrid system (BD Biosciences Clontech) according to the manufacturer's instructions. The bait plasmid, pGBKT7-ΔSAF-box, was transformed into *Saccharomyces cerevisiae* AH109 and used to screen the pretransformed *S. cerevisiae* Y187 (BD Biosciences Clontech) containing a human liver cDNA library constructed in the pACT2 plasmid. The mated cells were selected on high-stringency plates lacking adenine, histidine, leucine and tryptophan (QDO plates). Positive diploid cells that grew on the QDO plates were tested for both α- and β-galactosidase (BD Biosciences Clontech and Pierce, respectively) activities according to the manufacturers' recommendations. The β-galactosidase assay was performed in triplicate. Plasmids from the positive cells were extracted, sequenced and co-transformed together with pGBKT7-ΔSAF-box back into *S. cerevisiae* AH109 to verify the interactions.

GST pull-down assay

Approximately 10 µg GST or GST-Hcc-1 that were immobilized on the glutathione-agarose beads (Sigma) was mixed with 10 µg 6 × His-BAT1 or 6 × His-DDX39 in a binding buffer (150 mM NaCl, 10 mM Tris, pH 8.0, 0.3% Igepal, 1 mM DTT, 0.5 mM PMSF) and incubated at 4 °C for 3 h. The mixtures were washed three times in the same binding buffer. Bound proteins were boiled in 2 × sample buffer (0.12 M Tris, pH 6.8, 0.2% glycerol, 4% SDS, 0.01% bromophenol-blue, 10 mM DTT), separated by SDS-PAGE, electroblotted onto a nitrocellulose membrane (Amersham Biosciences) and probed with anti-His (Qiagen) antibody.

Co-immunoprecipitation assay

HEK293 cells overexpressing Hcc-1 were transfected with either pCMV-myc-DDX39 or pCMV-myc-BAT1 expression vectors for 48 h. Transfected cells (1×10^7) were then lysed in a lysis buffer (50 mM Tris-Cl, pH 7.4, 150 mM NaCl, 0.5% Triton X-100) and the lysate was incubated with a 50% slurry of Protein A or G (KPL) beads for 1 h at 4 °C. The precleared cell extract was incubated with 5 µg anti-myc monoclonal antibody (BD Biosciences Clontech) and protein G, or 5 µl anti-Hcc-1 antiserum and protein A at 4 °C overnight. The beads were washed three times with the lysis buffer and resuspended in a 2 × sample buffer. Bound proteins were resolved by SDS-PAGE and detected after Western blotting using the anti-myc antibody and the anti-Hcc-1 antiserum. Preimmunized rabbit serum and unrelated mouse monoclonal antibody were used as negative controls. Protein A or G were used as mock samples.

Western blot analysis

Following electrophoresis, proteins were transferred from the SDS-polyacrylamide gel to a nitrocellulose membrane (Amersham Biosciences). Non-specific sites were blocked with a blocking reagent (5% skim milk in $TBST_{20}$) and the membrane was incubated with a primary antibody (diluted 1:1000 in 1% skim milk in $TBST_{20}$). Horseradish peroxidase-conjugated secondary antibody (diluted 1:10,000 in 1% skim milk in $TBST_{20}$) was subsequently added to the membrane and the horseradish peroxidase activity was detected using the SuperSignal West Pico chemiluminescent substrate (Pierce) with protocols provided by the manufacturer.

Tissue distribution profiles of BAT1 and DDX39

The cDNA distributions of *BAT1* and *DDX39* genes were screened by semi-quantitative PCR on a normalized human multiple-tissue cDNA panel (BD Biosciences Clontech). The cDNA expression profile in a tumor and its adjacent non-tumor liver tissue from a subject with HCC were also examined. DNA primers for *BAT1* and *DDX39* were synthesized (Proligo) based on sequence information published in GenBank. A housekeeping gene, glyceraldehyde-3-phosphate dehydrogenase, was used as control in the amplification. The PCR mixture consisted of 5 µl of the first-strand cDNA from the tissue panel, 0.2 mM deoxyribonucleotides, 1.5 mM $MgCl_2$, 0.2 µM of each primer and 0.5 U Taq polymerase (Promega) in a reaction buffer from the same manufacturer. The semi-

quantitative cycling parameters were 94 °C for 1 min, followed by 20–34 cycles of 94 °C for 30 s, 58 °C for 30 s, 72 °C for 1 min. This was to determine the presaturation linear amplification cycles, and the midpoint of the linear amplification was chosen for semi-quantitative analysis. PCR products were examined by electrophoresis on a 1% agarose gel.

Generation of a stably transfected HEK293 cell line expressing Hcc-1

HEK293 cells were cultured in Dulbecco's modified Eagle's medium (DMEM, Gibco BRL) supplemented with 10% fetal bovine serum (FBS) (Gibco BRL) at 37 °C in a humidified atmosphere containing 5% CO_2. The plasmids pcDNA3.1(+)-Hcc-1 and pcDNA3.1(+) were transfected separately into HEK293 cells using the Lipofectamine (Invitrogen) reagent according to the manufacturer's protocol. Stably transfected clones were cultured in 200 µg/ml geneticin (Invitrogen). Expression of Hcc-1 was determined by Western blot.

Cell proliferation assays

For the viable-cell counting assay, stably transfected and parental HEK293 cells were seeded in triplicate at 0.5×10^6 cells per well in six-well tissue culture plates with 3%, 5% or 10% FBS in DMEM. The number of viable cells was counted at 24, 48, 72 and 96 h after seeding. Cell cycle analysis was performed by seeding cells in duplicate at 0.5×10^6 per well in DMEM supplemented with 10% FBS and growth for 48 h. The percentage of cells in each stage of the cell cycle was determined by flow cytometry using the CycleTEST PLUS DNA reagent kit (Becton-Dickinson), and analyzed using the CellQuest and ModFIT LT V2.0 software (Becton-Dickinson). For the BrdU incorporation assay, transfected cells were seeded in quadruplicate in a 96-well microtiter plate and grown for 48 h at 37 °C. The amount of incorporated BrdU was then determined as recommended by the manufacturer (Roche Molecular Biochemicals). Statistical analysis was performed using Student's t test.

Results

Hcc-1 exhibits nucleic acid-binding ability and binds specifically to SAR DNA

The presence of the putative SAF-box DNA-binding motif at the N terminal of Hcc-1 prompted us to study its nucleic acid-binding ability. GST-Hcc-1 and GST-ΔSAF-box were able to bind to both dsDNA and ssDNA (fig. 1), although full-length Hcc-1 bound to ssDNA with higher affinity. Both GST-Hcc-1 and GST-ΔSAF-box showed weak affinities to dsDNA as no proteins were retained in the column after 0.25 M NaCl elution. GST and GST-SAF-box did not bind to the DNA columns, being completely eluted during the washing steps (results not shown). The binding specificity of Hcc-1 was further elucidated using SAR DNA. As shown in figure 2, binding of the MII SAR DNA to Hcc-1 was still detectable even in the presence of a 10,000-fold higher concentration of sheared *E. coli* DNA. Furthermore, binding of Hcc-1 to MII was not affected by the presence of a GC-specific competitor, chromomycin. However, the binding was abolished with increasing concentrations of poly dA-dT and an AT-specific competitor, distamycin. These findings indicate that Hcc-1 has a specific affinity for single-stranded and AT stretch DNA sequences. The binding of various Hcc-1 deletion constructs to SAR DNA was studied. The GST-SAF-box construct did not bind to the SAR DNA, while the GST-ΔSAF-box showed similar binding capability to SAR DNA as the full-length GST-Hcc-1 (results not shown).

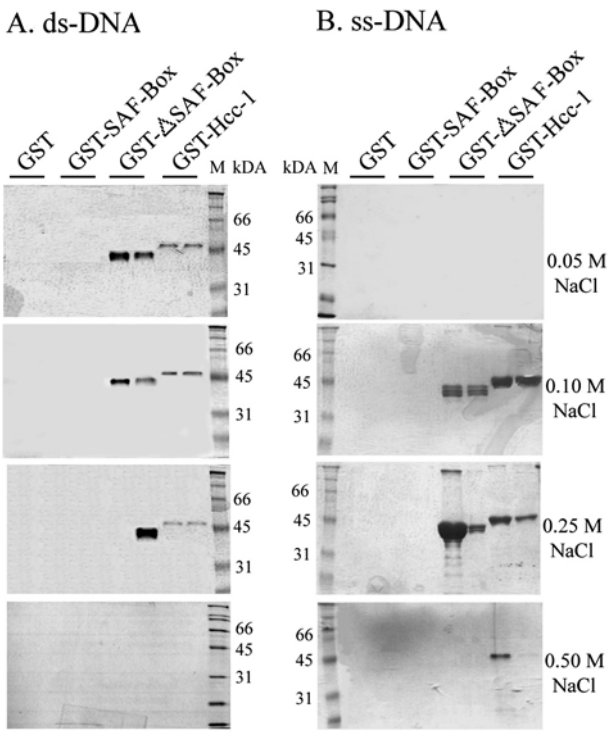

Figure 1. Hcc-1 exhibits nucleic acid-binding ability. Salt elution profiles of Hcc-1 constructs from ds (*A*) and ss (*B*) calf thymus DNA cellulose. Hcc-1 was retained in the ssDNA column up to a concentration of 0.5 M NaCl while it was completely eluted from the dsDNA column at the same NaCl concentration. This showed that Hcc-1 has a higher affinity for ssDNA. GST and GST-SAF-box did not bind to the columns, and were completely eluted out during the washing steps.

Hcc-1 interacts with the DEAD-box proteins BAT1 and DDX39

The yeast two-hybrid assay was used to identify partner proteins of Hcc-1. A human liver cDNA library was used in this approach because Hcc-1 was initially identified in

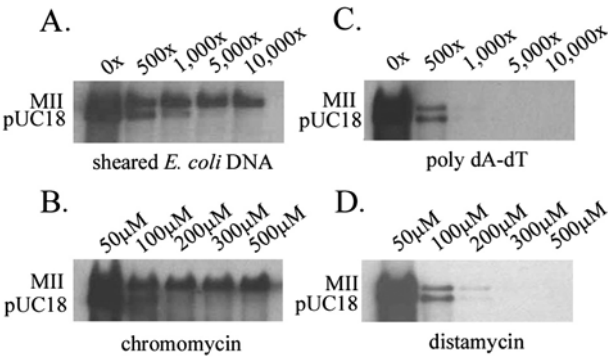

Figure 2. Hcc-1 binds specifically to SAR DNA. A DIG-labeled MII fragment was incubated with purified GST-Hcc-1 protein coupled to GST beads. Binding of the MII fragment (250 ng) to Hcc-1 was not affected by increasing concentrations of non-specific sheared *E. coli* DNA (*A*) or the GC-specific competitor, chromomycin (*B*). However, the binding was abolished with increasing concentrations of poly dA-dT (*C*) and the AT-specific competitor, distamycin (*D*). The quantity of sheared *E. coli* DNA and poly dA-dT used in the experiment was measured as folds above the quantity of the input MII fragment (250 ng).

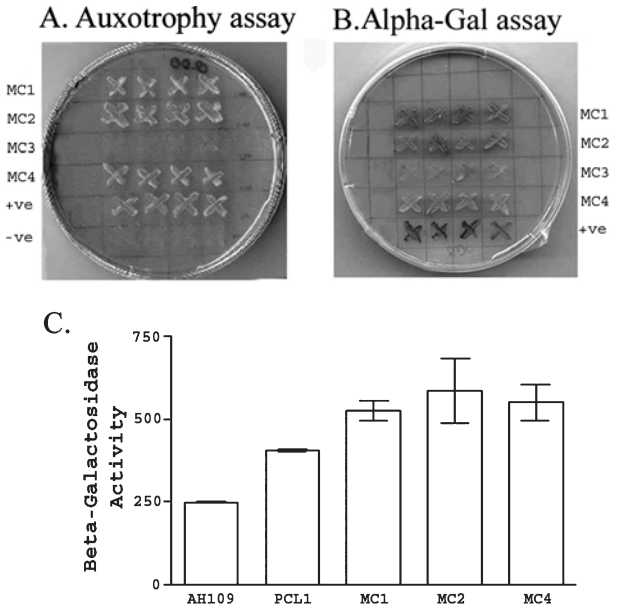

Figure 3. Four-mated clones from the yeast two-hybrid assay. Except for clone MC3, all positive co-transformant clones were able to grow on the QDO plate (*A*) and showed α-galactosidase activities (*B*). MC1, MC2 and MC4 also demonstrated β-galactosidase activities (*C*). PCL1 is a positive control (for α- and β-galactosidase assays) strain containing a plasmid coding for *Mel1* and *LacZ* genes.

the HCC-M cell line and in well-differentiated HCC tissues. Approximately 5×10^6 clones were screened and four Ade^+/His^+ (both reporter genes were activated) isolates were obtained. We named the four isolates MC1, MC2, MC3 and MC4. Except for MC3, the other three isolates were positive for both α- and β-galactosidase activities (activation of *Mel1* and *LacZ* genes, respectively) and were able to regrow on QDO plates (activation of *Ade* and *His* genes). To confirm the interactions, the cDNA library plasmids from the four isolates were rescued in *E. coli* and co-transformed into AH109 yeast cells together with the pGBKT7-ΔSAF-box bait plasmid. Except for the plasmid isolated from MC3, all co-transformant clones were able to activate the reporter genes (*Ade*, *His*, *LacZ* and *Mel1*) (fig. 3). We then performed DNA sequencing analysis to identify the four clones. BLAST searches of the DNA sequences from MC1 and MC2 showed that they were identical and aligned with the *DDX39* gene (GenBank Accession number NM_005804). NCBI BLAST searches of MC4 showed that it aligned with the *BAT1* gene (GenBank Accession number NM_004640) while MC3 is a truncated version of MC4 with approximately 200 bp missing from the 5′ end of the *BAT1* gene.

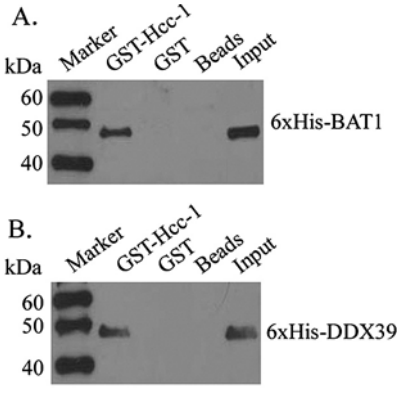

Figure 4. Hcc-1 interacts in vitro with BAT1 and DDX39. Purified 6 × His-BAT1 (*A*) or 6 × His-DDX39 (*B*) (at 10 μg) was incubated with an equal amount of GST or GST-Hcc-1 coupled to glutathione-agarose beads. In vitro binding of 6 × His-BAT1 and DDX39 to GST-Hcc-1 was detected with anti-His antibody. Purified 6 × His-tagged BAT1 or DDX39 were used as positive controls (Input lane) for the antibody detection step.

In vitro and in vivo interactions between Hcc-1 and the DEAD-box proteins

The interactions suggested by the yeast two-hybrid assay were further confirmed by a GST pull-down assay. Full-length BAT1 and DDX39 were expressed as 6 × His tag fusion proteins and mixed with GST-Hcc-1 protein. The immunoblot analysis showed that both 6 × His-BAT1 and 6 × His-DDX39 bound to GST-Hcc-1 in vitro (fig. 4). No binding was observed between 6 × His-BAT1 or 6 × His-DDX39 with the GST protein alone, or with the empty glutathione-agarose beads. Co-immunoprecipitation assays were then performed to confirm the interactions in vivo. The transfected cell lysates were incubated with either anti-myc or anti-Hcc-1 antibodies and purified using protein A or G agarose beads, respectively. As shown in figure 5, myc-DDX39 and myc-BAT1 were co-immunoprecipitated with Hcc-1, and vice versa. The co-immuno-

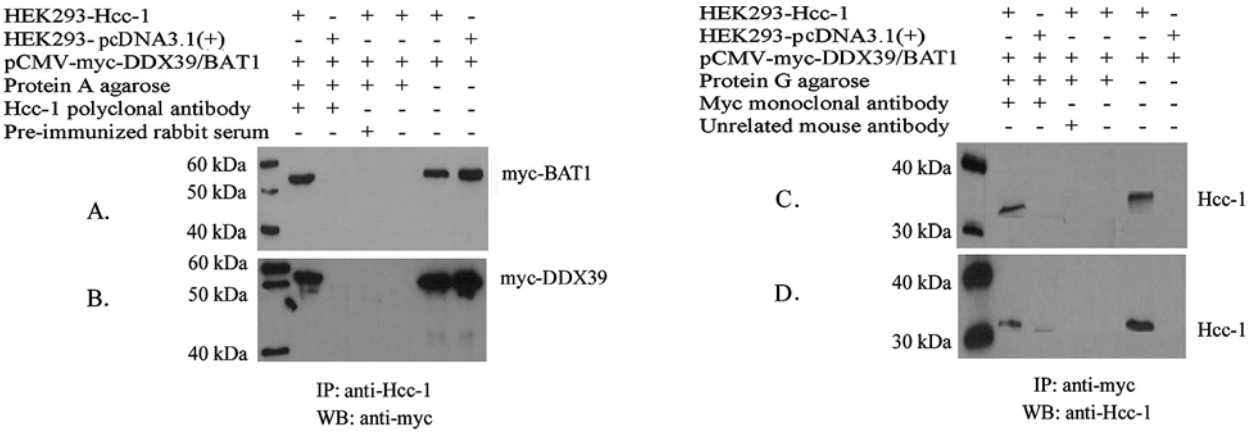

Figure 5. Hcc-1 interacts in vivo with BAT1 and DDX39. Cell lysate overexpressing Hcc-1 and myc-BAT1 (*A, C*) or Hcc-1 and myc-DDX39 (*B, D*) were immunoprecipitated with either anti-Hcc-1 or anti-myc antibodies. The immunoprecipitates were detected with anti-myc (*A, B*) and anti-HCC-1 (*C, D*) antibodies.

precipitation results further confirmed that BAT1 and DDX39 were proteins that associated physically with Hcc-1 in vivo.

Tissue distribution profiles of BAT 1 and DDX39

A semi-quantitative PCR method was chosen to study the distribution profiles of *BAT1* and *DDX39* in various human tissues. This method was chosen over the conventional Northern blot method because it permits detection of mRNA of all abundance levels and is much faster than hybridization analyses. A trial PCR experiment was performed to 20–34 cycles with two-cycle intervals. An aliquot of the PCR mixture at each interval was electrophoresed on a 1% ethidium bromide-stained agarose

Table 1. Semi-quantitative PCR analysis of *Hcc-1*, *BAT1* and *DDX39* cDNA levels in human tissues.

Tissue types	Samples	*Hcc-1*	*BAT1*	*DDX39*
Healthy tissue	colon	–	–	–
	ovary	–	–	–
	peripheral blood leukocyte	–	–	–
	prostate	+/–	+/–	+/–
	small intestine	–	+/–	+/–
	spleen	+	+	+
	testis	++	+	++
	thymus	+	+/–	+/–
	brain	–	–	–
	heart	+	+	+/–
	kidney	+	+	+/–
	liver	+/–	+	+/–
	lung	–	–	–
	pancreas	+	+	+/–
	placenta	–	+	+/–
	skeletal muscle	–	–	–
Disease tissue	breast carcinoma	+/–	+/–	–
	lung carcinoma	–	–	–
	colon adenocarcinoma	–	–	–
	lung carcinoma	–	–	–
	prostatic adenocarcinoma	–	–	–
	colon adenocarcinoma	–	–	–
	ovarian carcinoma	–	–	+/–
	pancreatic adenocarcinoma	+++	++	+/–
Paired liver samples	non-tumor tissue cDNA	++	++	–
	adjacent tumor tissue cDNA	+	+	+

The semi-quantitative analysis was performed at cycle 26. Relative expression levels are based on the relative brightness of the ethidium bromide-stained DNA bands on the agarose gel where +++ > ++ > + > +/–, and – denotes no expression. cDNA from paired liver samples was derived from an HCC patient with hepatitis B infection who had poorly differentiated tumor cells.

gel. The exponential phase of the PCR was determined visually and found to range from 22 to 30 cycles. Saturation was found to begin after cycle 32. We chose to stop the PCR at cycle 26 for the semi-quantitative analysis of the cDNA levels of the various genes. The non-saturating PCR on the normalized starting single-stranded cDNA tissue panel should give an accurate comparison of relative mRNA copy numbers [19, 20]. *Hcc-1* and *BAT1* had a similar transcript profile in most of the tissues investigated (table 1). This suggests that *BAT1* is co-expressed with *Hcc-1*. The expression of *DDX39* was observed to be low in all tissue types investigated. The expression levels of *Hcc-1*, *BAT1* and *DDX39* were also examined in a tumor and its adjacent normal tissues derived from the liver of a subject with poorly differentiated HCC. Similar to *Hcc-1*, *BAT1* was expressed in both tumor and non-tumor cells but with a higher transcript level in the non-tumor tissue. In contrast, *DDX39* was undetectable in the non-tumor tissue; it was only observed in the tumor tissue (table 1).

Expression of Hcc-1 affects cell growth

The HEK293 cell line does not express Hcc-1 as determined by reverse transcription-PCR using Hcc-1-specific primers (results not shown) and Western blot (figs 6 and 7).

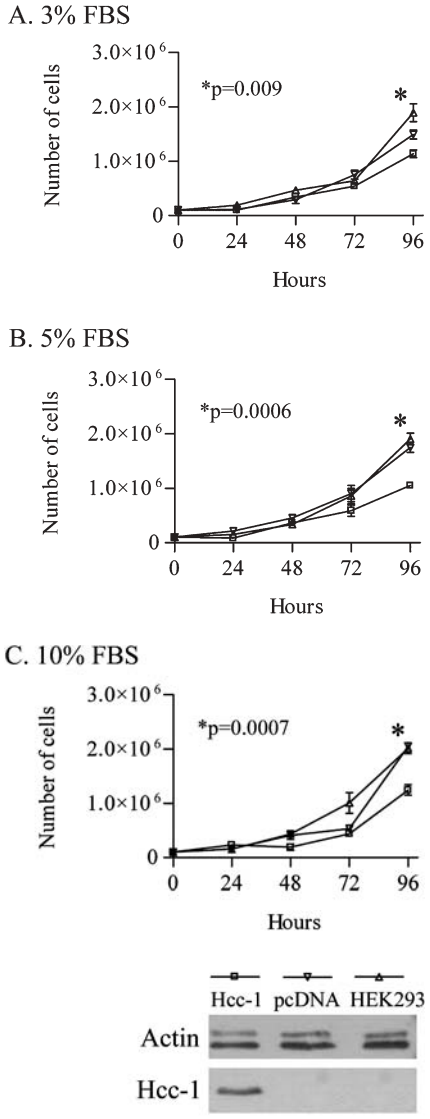

Figure 6. HEK293 cells overexpressing Hcc-1 have a slower growth rate. Cells were seeded in triplicate at 5×10^5 per well with 3% (*A*), 5% (*B*) and 10% (*C*) FBS, and cultured for up to 96 h. The number of cells was counted at 24, 48, 72 and 96 h. Data shown here are from a representative experiment. Western blots of actin and Hcc-1 are shown to illustrate the relative expression of these proteins in the three cell types.

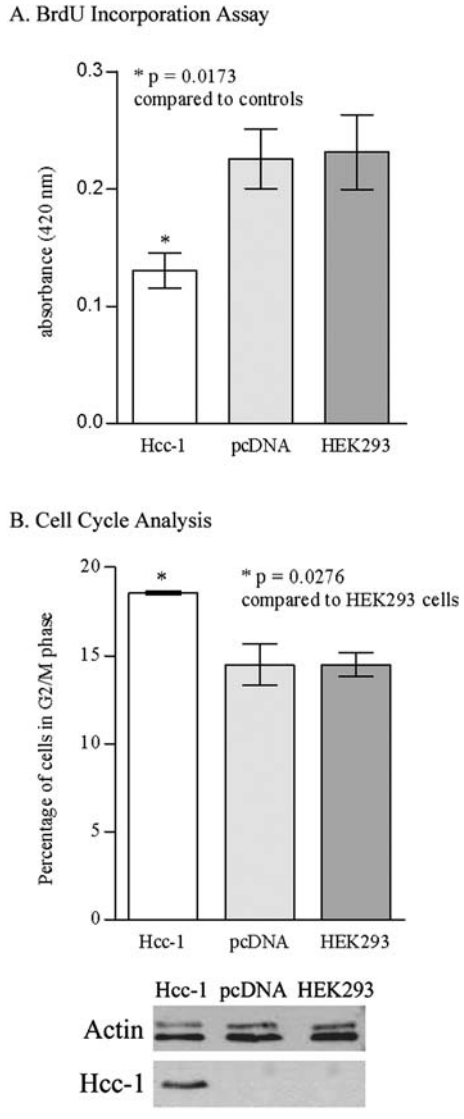

Figure 7. HEK293 cells overexpressing Hcc-1 have a reduced BrdU incorporation rate by 40% ($p = 0.017$) (*A*) and increased accumulation of cells at the G2/M phase by 28% ($p = 0.0276$) (*B*) compared to controls. The experiments were carried out in duplicate after growing the HEK293-Hcc-1 subline and controls for 48 h. Western blots of actin and Hcc-1 are shown to illustrate the relative expression of these proteins in the three cell types.

Thus the effect of expressing Hcc-1 in this cell line should be readily observed. A stably transfected HEK293 subline expressing Hcc-1 was generated. The expression level of Hcc-1 in this subline is shown in figures 6 and 7. The cell count study showed that the cell density of the HEK293 subline expressing Hcc-1 was significantly lower compared to the two controls (HEK293 cell line and pcDNA3.1(+)-transfected subline) at every time point under the nutrient stress conditions (3% and 5% FBS at $p = 0.009$ and $p = 0.0006$, respectively), as well as in the normal culture condition (10% FBS at $p = 0.0007$) (fig. 6). In addition, the BrdU incorporation rate was significantly lowered by 40% ($p = 0.0173$) in the Hcc-1-expressing subline as compared to the controls (fig. 7). Flow cytometry analysis showed that the percentage of Hcc-1-expressing cells in the G2/M phase increased significantly by 28% ($p = 0.0276$) compared to the control HEK293 cells 48 h after plating (fig. 7). A corresponding drop in the percentage of cells in S phase (by 20%) was also observed. This is in concordance with findings from the BrdU incorporation assay where the number of replicating cells in S phase was lower in the Hcc-1-expressing subline.

Discussion

We showed that the recombinant GST-Hcc-1, as well as native Hcc-1 (data not shown), were able to bind to both dsDNA and ssDNA cellulose. This indicates that Hcc-1 has a general nucleic acid-binding ability. The finding that GST-Hcc-1 was retained in the ssDNA cellulose column up to an NaCl concentration of 0.5 M, whereas nearly all bound GST-Hcc-1 and GST-ΔSAF-box were eluted from the dsDNA cellulose column at 0.25 M NaCl, suggests that full-length Hcc-1 has a higher affinity for ssDNA. The nucleic acid-binding ability of GST-ΔSAF-box and GST-Hcc-1 were not due to the GST fusion protein since GST protein alone did not bind to either ssDNA or dsDNA cellulose columns. The SAF-box has no nucleic acid-binding activity since the GST-SAF-box was eluted entirely from both ds- and ssDNA cellulose columns. The binding of a single SAF-box to DNA has been reported to be unstable and of low affinity [4]. On the other hand, GST-ΔSAF-box seemed to possess nucleic acid-binding ability even though there is no known DNA-binding domain/motif on this peptide fragment. The binding mechanism of GST-ΔSAF-box to both the ss- and dsDNA celluloses is not clear from the present study. One possible explanation is the presence of yet unknown DNA/RNA-binding motifs at this region, as the SAF-box always tethers other domains involved in pre-mRNA processing [3].

The binding of Hcc-1 to SAR DNA was observed to be highly specific. Our results showed that the binding was still detectable in the presence of high concentrations of the non-specific competitors, chromomycin and sheared *E. coli* DNA. In contrast, the binding of Hcc-1 to the MII SAR DNA was undetectable in the presence of specific competitors such as poly-dA-dT and distamycin. The specific binding of Hcc-1 toward AT-rich DNA implies that it may be an S/MAR-binding protein. S/MAR-binding proteins, such as NMPs and hnRNPs, are abundant proteins in the nuclear scaffold. They are required for the maintenance of the internal nuclear architecture [21]. In general, hnRNPs also bind well to both RNA and ssDNA but show weaker affinity for dsDNA [10]. Beside maintaining the chromatin architecture, some S/MAR-binding proteins (for example SATB1, SAF-B and histone H1) may fulfill more specialized roles in scaffold-related functions such as transcription, splicing, DNA replication and DNA repair [22]. SAF-A/hnRNP U binds to dsDNA, ssDNA and SAR DNA. It is also involved in the packaging and processing of RNA, with a suggested role in RNA metabolism, chromatin organization and nuclear architecture [9–11]

From the yeast two-hybrid, GST pull-down and co-immunoprecipitation assays, we showed that Hcc-1 associates with BAT1 and DDX39. Both BAT1 and DDX39 share 89% homology at the amino acid sequence level but are encoded by two different genes. BAT1 and DDX39 belong to the DEAD-box family that is characterized by having seven to eight conserved motifs including RNA-unwinding and ATP hydrolysis motifs. In addition, the N- and C-terminal extensions of DEAD-box proteins are required for cellular localization, protein-protein and protein-RNA interactions [23, 24]. The MC3 clone, which has the same cDNA sequence as *BAT1* but with a 200-bp deletion at the 5′ end, yielded inconsistent results in the yeast two-hybrid assay. This suggests that the missing region is essential for protein-protein interaction.

DEAD-box proteins are ATP-dependent RNA helicases. They interact with hnRNPs to facilitate the biogenesis of mRNA such as pre-mRNA processing and mRNA transport by forming a complex of spliceosome assembly [25, 26]. The spliceosome complex is also comprised of SAF-box proteins and other NMPs [17, 27]. Further evidence for the coupling of a chromatin-organizing SAR DNA-binding element such as Hcc-1 to transcriptional regulation and pre-mRNA processing came from a study on the SAF-B protein [28]. SAF-B, which specifically binds to SAR regions, was shown to interact with RNA polymerase II and a subset of serine-/arginine-rich RNA-processing factors known as SR proteins. This indicates an association of SAR DNA-binding elements with the transcription machinery and the formation of a ‘transcriptosome complex’ in the vicinity of actively transcribed genes [28].

The cDNA expression patterns of *BAT1* are similar to those of *Hcc-1*, suggesting that BAT1 is co-expressed with Hcc-1 and may be functionally related. Interestingly, de-

spite having high protein homology with BAT1, DDX39 was hardly detectable in all the tissues investigated. We showed that expression of Hcc-1 in HEK293 cells inhibited cell proliferation significantly. Expression of BAT1 is also reported to be associated with proliferation inhibition, which may be blocked by DDX39 [29]. Our findings that BAT1 had higher expression in the normal liver tissue while DDX39 was only observed in the tumor tissue further confirmed the above report. Thus, interactions between Hcc-1 and BAT1 may be a normal body defense mechanism whereby cells limit their proliferation rate. BAT1 is inhibited when expression of DDX39 increases, and this leads to an increase in cell proliferation which may subsequently contribute to oncogenesis.

We showed that Hcc-1 possesses similar nucleic acid-binding characteristics to hnRNPs by binding to SAR DNA with high specificity and to ssDNA (with weaker affinity for dsDNA). Furthermore, Hcc-1 has a scattered distribution pattern in the nucleus [1] similar to the distribution patterns of other hnRNPs, including those capable of binding to SARs [30]. Taking these results into consideration, Hcc-1 may be a novel NMP or hnRNP with a function in nuclear architecture, and in nucleic acid metabolism and biogenesis. Interactions with the two DEAD-box proteins, BAT1 and DDX39, further support a role for Hcc-1 in nucleic acid biogenesis. Future studies on the influence of Hcc-1 in RNA processing in relation to the concept of a transcriptosome will be of particular interest. Expression of Hcc-1 in cells led to growth inhibition, consistent with the property of its interacting partner, BAT1. The differential expression of BAT1 and DDX39 may suggest that both proteins interact with Hcc-1 at different stages of cellular events, with the Hcc-1-BAT1 complex possibly acting as a negative regulator to inhibit cell proliferation. The precise molecular mechanism of Hcc-1 action in growth suppression warrants further studies in view of these interesting findings as a potential growth inhibitor.

Acknowledgements. All experimental work was carried out at the Bioprocessing Technology Institute. The authors thank Dr N. Cheong, Ms A. Tan, Ms A. Teo, Ms C. Liang, Mr J. D. A. Ramos, Mr S. M. Yeoh, Ms S. L. Lo and Ms C. Y. Chu for their precious advice, support and discussion. We are grateful to Prof. F. O. Fackelmayer for providing the MII-pUC18 plasmid.

1 Choong M. L., Tan L. K., Lo S. L., Ren E.-C., Ou K., Ong S. E. et al. (2001) An integrated approach in the discovery and characterization of a novel nuclear protein over-expressed in liver and pancreatic tumors. FEBS Lett. **496:** 109–116
2 Fukuda S., Wu D. W., Stark K. and Pelus L. M. (2002) Cloning and characterization of a proliferation-associated cytokine-inducible protein, CIP29. Biochem. Biophys. Res. Commun. **292:** 593–600
3 Aravind L. and Koonin E. V. (2000) SAP – a putative DNA-binding motif involved in chromosomal organization. Trends Biochem. Sci. **25:** 112–114
4 Kipp M., Göhring F., Ostendorp T., Drunen C. M. van, Driel R. van, Przybylski M. et al. (2000) SAF-box, a conserved protein domain that specifically recognizes scaffold attachment region DNA. Mol. Cell. Biol. **20:** 7480–7489
5 Renz A. and Falkelmayer F. O. (1996) Purification and molecular cloning of the scaffold attachment factor B (SAF-B), a novel human nuclear protein that specifically binds to s/MAR-DNA. Nucleic Acids Res. **24:** 843–849
6 Sahara S., Aoto M., Eguchi Y., Imamoto N., Yoneda Y. and Tsujimoto Y. (1999) Acinus is a caspase-3-activated protein required for apoptotic chromatin condensation. Nature **401:** 168–173
7 Tan J., Hall S. H., Hamil K. G., Grossman G., Petrusz P., Liao J. et al. (2000) Protein inhibitor of activated STAT-1 (signal transducer and activator of transcription-1) is a nuclear receptor coregulator expressed in human testis. Mol. Endocrinol. **14:** 14–26
8 Sasazuki T., Sawada T., Sakon S., Kitamura T., Kishi T., Okazaki T. et al. (2002) Identification of a novel transcriptional activator, BSAC, by a functional cloning to inhibit TNF-induced cell death. J. Biol. Chem. **277:** 28853–28860
9 Kiledjian M. and Dreyfuss G. (1992) Primary structure and binding activity of the hnRNP U protein: binding RNA through RGG box. EMBO J. **11:** 2655–2664
10 Fackelmayer F. O. and Richter A. (1994) Purification of two isoforms of hnRNP-U and characterization of their nucleic acid binding activity. Biochemistry **33:** 10416–10422
11 Fackelmayer F. O., Dahm K., Renz A., Ramsperger U. and Richter A. (1994) Nucleic-acid-binding properties of hnRNP-U/SAF-A, a nuclear-matrix protein which binds DNA and RNA in vivo and in vitro. Eur. J. Biochem. **221:** 749–757
12 Romig H., Fackelmayer F. O., Renz A., Ramsperger U. and Richter A. (1992) Characterization of SAF-A, a novel nuclear DNA-binding protein from HeLa cells with high affinity of nuclear matrix/scaffold attachment DNA elements. EMBO J. **11:** 3431–3440
13 Jenuwein T., Forrester W. C., Fernandez-Herrero L. A., Laible G., Dull M. and Grosschedl R. (1997) Extension of chromatin accessibility by nuclear matrix attachment regions. Nature **385:** 269–272
14 Gasser S. M. and Laemmli U. K. (1986) Cohabitation of scaffold binding regions with upstream/enhancer elements of three developmentally regulated genes of *D. melanogaster*. Cell **46:** 521–530
15 Hamm J. and Lamond A. I. (1998) Spliceosome assembly: the unwinding role of DEAD-box proteins. Curr. Biol. **8:** R532–R534
16 Reed R. (2000) Mechanisms of fidelity in pre-mRNA splicing. Curr. Opin. Cell Biol. **12:** 340–345
17 Hartmuth K., Urlaub H., Vornlocher H.-P., Will C. L., Gentzel M., Wilm M. et al. (2002) Protein composition of human prespliceosomes isolated by a tobramycin affinity-selection method. Proc. Natl. Acad. Sci. USA **99:** 16719–16724
18 Romig H., Ruff J., Falkelmayer F. O., Patil M. S. and Richter A. (1994) Characterization of two intronic nuclear-matrix-attachment regions in the human DNA topoisomerase I gene. Eur. J. Biochem. **221:** 411–419
19 Spanakis E. and Brouty-Boye D. (1994) Evaluation of quantitative variation in gene expression. Nucleic Acids Res. **22:** 799–806
20 Savonet V., Mainhaut C., Miot F. and Pirson I. (1997) Pitfalls in the use of several 'housekeeping' genes as standards for quantitation of mRNA: the example of thyroid cells. Anal. Biochem. **247:** 165–167
21 He D. C., Nickerson J. A. and Penman S. (1990) Core filaments of the nuclear matrix. J. Cell Biol. **110:** 569–580
22 Galande S., Dickinson L. A., Mian I. S., Sikorska M. and Kohwi-Shigematsu T. (2001) SATB1 cleavage by caspase 6 disrupts PDZ domain-mediated dimerization, causing detachment

form chromatin early in T-cell apoptosis. Mol. Cell Biol. **21:** 5591–5604
23 Wang Y. and Guthrie C. (1998) PRP16, a DEAD-box RNA helicases, is recruited to the spliceosome primarily via its nonconserved N-terminal domain. RNA **4:** 1216–1229
24 Linder P. and Daugeron M. C. (2000) Are DEAD-box proteins becoming respectable helicases? Nat. Struct. Biol. **7:** 97–99
25 Gorlach M., Burd C. G., Portman D. S. and Dreyfuss G. (1993) The hnRNP proteins. Mol. Biol. Rep. **18:** 73–78
26 Linder P. and Stutz F. (2001) mRNA export: traveling with DEAD box proteins. Curr. Biol. **11:** R961–R963
27 Blencowe B. J., Nickerson J. A., Issner R., Penman S. and Sharp P.A. (1994) Association of nuclear matrix antigens with exon-containing splicing complexes. J. Cell Biol. **127:** 593–607
28 Nayler O., Strätling W., Bourquin J.-P., Stagljar I., Lindemann L., Jasper H. et al. (1998) SAF-B protein couples transcription and pre-mRNA splicing to SAR/MAR elements. Nucleic Acids Res. **26:** 3542–3549
29 Allcock R .J., Wiliams J. H. and Price P. (2001) The central MHC gene, BAT1, may encode a protein that down-regulates cytokine production. Genes Cells. **6:** 487–494
30 Mattern K.A., Humbel B. M., Muijsers A. O., Jong L. de and Driel R. van (1996) hnRNP proteins and B23 are the major proteins of the internal nuclear matrix of HeLa S3 cells. J. Cell Biochem. **62:** 275–289